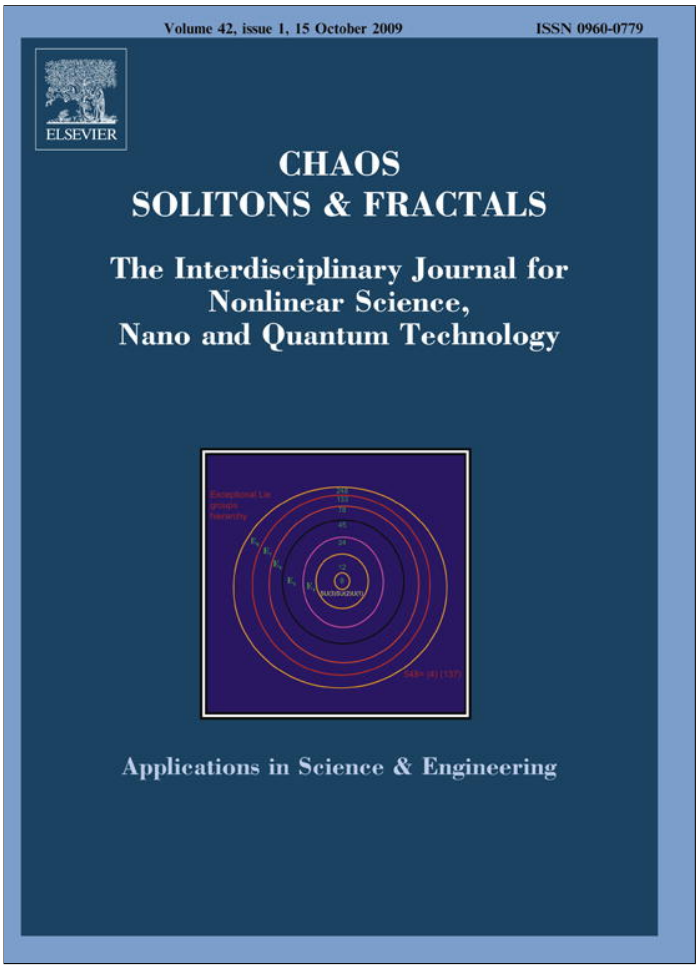

Chaos, Solitons and Fractals 42 (2009) 155–169

Contents lists available at ScienceDirect

Chaos, Solitons and Fractals

journal homepage: www.elsevier.com/locate/chaos

The effect of J_2 on equatorial and halo orbits around a magnetic planet

Manuel Iñarrea [a], Víctor Lanchares [b,*], Jesús F. Palacián [c], Ana I. Pascual [b], J. Pablo Salas [a], Patricia Yanguas [c]

[a] Universidad de la Rioja, Área de Física, 26006 Logroño, Spain
[b] Dpto. de Matemáticas y Computación, CIEMUR: Centro de Investigación en Informática, Estadística y Matemáticas, Universidad de la Rioja, 26004 Logroño, Spain
[c] Universidad Pública de Navarra, Departamento de Ingeniería Matemática e Informática, 31006 Pamplona, Spain

ARTICLE INFO

Article history:
Accepted 12 November 2008

ABSTRACT

We calculate equatorial and halo orbits around a non-spherical (both oblate and prolate) magnetic planet. It is known that circular equatorial and halo orbits exist for a dust grain orbiting a spherical magnetic planet. However, the frequency of the orbit is constrained by the charge–mass ratio of the particle. If the non-sphericity of the planet is taken into account this constraint is modified or, in some cases, it disappears.

1. Introduction

The dynamics of a test body orbiting another one under the action of several disturbing forces is derived from the so called perturbed Keplerian systems. If the perturbation is small enough, the motion of the test body is expected to be close to the unperturbed one, given by the classical orbits of the two body problem. However, for some particular systems, special type of non-Keplerian orbits can appear. This is the case of circular orbits lying in a plane perpendicular to the z-axis within a measurable distance to the equatorial plane. They are the halo orbits and have been reported in several problems. For instance, in the classical problem of the movement of an artificial satellite, when the two first dominant terms in the gravitational potential are considered, if the attracting body is prolate [17]. They also appear in the problem of the movement of a charged dust particle orbiting a magnetic planet [4,10,11].

The two problems can be combined and, with the influence of radiation pressure, we arrive at a realistic model to study the motion of charged dust grains into the electromagnetic ambient of giant planets. This model has been already considered by several authors for the study of dusty rings, like the E ring in Saturn [6,7,9,12]. By numerical simulations, it is proved that the model in [4,10,11], where the planet is supposed to be spherical and there is no radiation pressure, gives rise to a dynamics close to that of the full perturbed system, in the case of Saturn. In particular, orbits parallel or almost parallel to the equator are found [12].

In the present paper, we will consider the problem of a charged particle orbiting a non-spherical magnetic planet. The main goal will be to perform an analytic study of the influence of the parameters of the system in the existence/persistence of circular orbits parallel to the equator or lying in it. We will pay special attention to the role played by the oblateness coefficient J_2, regardless its sign, i.e. if the body is either oblate or prolate. Sometimes, to highlight the differences with limit cases (spherical planet, no charge), unusual big values of J_2 will be considered, as well as it is done in [2] for the main problem of artificial satellite.

The paper is structured as follows. In Section 2, we state the Hamiltonian corresponding to the problem at hand. Section 3 is devoted to establish the equilibrium solutions. In Section 4, we analyze the existence of equatorial orbits, whereas in

* Corresponding author.
E-mail address: vlancha@unirioja.es (V. Lanchares).

0960-0779/$ - see front matter © 2008 Elsevier Ltd. All rights reserved.
doi:10.1016/j.chaos.2008.11.016

Section 5 we consider halo orbits; pointing out the differences existing between the oblate ($J_2 > 0$) and prolate ($J_2 < 0$) cases. The concluding remarks appear in Section 6.

2. The model

Our starting point is a model derived by Dullin et al. [4], a generalization of the classical one corresponding to a particle subject to a magnetic dipole field [22,23]. It is known as the generalised Størmer problem and it describes the dynamics of a dust particle of mass m and charge q orbiting a rotating magnetic planet of mass M. In this model, the magnetic field of the planet is supposed to be a perfect magnetic dipole of strength μ aligned along the north–south poles of the planet. Moreover, the planet's magnetosphere is taken as a rigid conducting plasma which rotates with the same angular velocity Ω as the planet, in such a way that the charge q is subject to a corotational electric field. In this way, using cylindrical coordinates and momenta $(\rho, z, \phi, P_\rho, P_z, P_\phi)$ and assuming that the gravitational interaction is purely Keplerian, the generalised Størmer problem can be modeled by the following dimensionless two-degree-of-freedom Hamiltonian

$$\mathscr{H}_S = \frac{1}{2}\left(P_\rho^2 + P_z^2 + \frac{P_\phi^2}{\rho^2}\right) - \frac{1}{r} - \delta\frac{P_\phi}{r^3} + \frac{\delta^2}{2}\frac{\rho^2}{r^6} + \delta\beta\frac{\rho^2}{r^3}, \tag{1}$$

where lengths and time are expressed, respectively, in units of the planetary radius R and the Keplerian frequency $w_K = \sqrt{M/R^3}$ (Gaussian units). The variable $r = \sqrt{\rho^2 + z^2}$ stands for the distance of the charged particle to the center of mass of the planet.

As the system is invariant under rotations around the z-axis, P_ϕ is an integral of the system. Furthermore, Hamiltonian (1) depends on two external parameters δ and β, introduced in [13,14], which indicate, respectively, the ratio between the magnetic and the Keplerian interactions and the ratio between the electrostatic and the Keplerian interactions. Specifically, $\delta = \omega_c/w_K$, accounts for the charge–mass ratio (q/m), being ω_c the cyclotron frequency, and $\beta = \Omega/w_K$, thus $\beta > 0$. On the other hand, the system depends on the two internal parameters P_ϕ and $\mathscr{H}_S = \mathscr{E}$ (the energy).

Some interesting consequences can be derived from this model. For instance, Dullin et al. [4] and Howard et al. [10,11] provide a comprehensive view of circular orbits, reporting what kind of particles and what frequencies are expected for a given distance away from the planet. They speculate with the possibility of finding halo orbits around Saturn. Grotta-Ragazzo et al. [5] give a possible explanation of the origin of the spokes detected on Saturn's rings by a detailed analysis of bifurcations among circular equatorial orbits. Iñarrea et al. [13,14], by studying the global Keplerian dynamics, report a special circular orbit that can be responsible for the narrowing of dusty rings.

Now we will introduce the effect of the oblateness of the planet in the Hamiltonian function (1). A classical model for the non-sphericity of a planet is given by means of the J_2 term [20]. In this way, Hamiltonian (1) becomes

$$H = \frac{1}{2}\left(P_\rho^2 + P_z^2 + \frac{P_\phi^2}{\rho^2}\right) - \frac{1}{r} - \delta\frac{P_\phi}{r^3} + \frac{\delta^2}{2}\frac{\rho^2}{r^6} + \delta\beta\frac{\rho^2}{r^3} + 3J_2\frac{z^2}{2r^5} - \frac{J_2}{2r^3}, \tag{2}$$

where J_2 is a positive dimensionless parameter for an oblate planet, whereas it is negative for a prolate one. For example, in the case of Saturn, $J_2 = 0.016298$ [1]. It is worth noting that Hamiltonian (2) generalises the cases studied by Langbort [17] ($\delta = 0$) and by Dullin et al. [4] ($J_2 = 0$), as it is the purpose of this paper.

3. Equilibrium solutions

Circular periodic trajectories around the z-axis correspond to equilibria (ρ_0, z_0) in the rotating meridian plane ρ–z, i.e. they appear as the equilibrium points of the system

$$\dot\rho = \frac{\partial\mathscr{H}}{\partial P_\rho}, \quad \dot z = \frac{\partial\mathscr{H}}{\partial P_z}, \quad \dot P_\rho = -\frac{\partial\mathscr{H}}{\partial\rho}, \quad \dot P_z = -\frac{\partial\mathscr{H}}{\partial z},$$

or equivalently, they are the critical points of the effective potential U_{eff} in (2), that is

$$U_{\text{eff}} = \frac{P_\phi^2}{2\rho^2} - \frac{1}{r} - \delta\frac{P_\phi}{r^3} + \frac{\delta^2}{2}\frac{\rho^2}{r^6} + \delta\beta\frac{\rho^2}{r^3} + 3J_2\frac{z^2}{2r^5} - \frac{J_2}{2r^3}. \tag{3}$$

Following the procedure of Dullin et al. [4] and Howard et al. [10,11], in order to better interpret the results, instead of P_ϕ, we introduce in (3) the particle angular velocity ω,

$$\omega = \dot\phi = \frac{\partial\mathscr{H}}{\partial P_\phi} = \frac{P_\phi}{\rho^2} - \frac{\delta}{r^3}.$$

The sign of ω determines if the motion of the particle is prograde (positive sign) or retrograde (negative sign) with respect to the planet. Besides, $\omega = \beta = \Omega$ represents a synchronous motion of the particle with the planet, thanks to the units of time chosen.

As a last change of variables, in order to simplify the calculations, we move to spherical variables (r, θ, ϕ), given by

$$\rho = r\sin\theta, \quad z = r\cos\theta,$$

with $\theta \in [0, \pi/2]$, due to the discrete symmetry $z \to -z$ of Hamiltonian (2). Now, the effective potential reads as

$$U_{\text{eff}} = -\frac{1}{r} + \delta\beta\frac{\sin^2\theta}{r} + \omega^2\frac{r^2\sin^2\theta}{2} + 3J_2\frac{\cos^2\theta}{2r^3} - \frac{J_2}{2r^3}. \tag{4}$$

The critical points of U_{eff} are found as the solutions of the system of equations

$$\begin{aligned}\frac{\partial U_{\text{eff}}}{\partial r} &= \frac{-3J_2}{r^4} + \frac{1}{r^2} + \left(\frac{9J_2}{2r^4} - \frac{\delta(\beta-\omega)}{r^2} - r\omega^2\right)\sin^2\theta = 0,\\ \frac{\partial U_{\text{eff}}}{\partial \theta} &= \left(-\frac{3J_2}{2r^3} + \frac{\delta(\beta-\omega)}{r} - \frac{r^2\omega^2}{2}\right)\sin 2\theta = 0.\end{aligned} \tag{5}$$

The above system gives rise to the equivalent non-linear system

$$\begin{aligned}&-6J_2 + 2r^2 + (9J_2 - 2\delta(\beta-\omega)r^2 - 2r^5\omega^2)\sin^2\theta = 0,\\ &(-3J_2 + 2\delta(\beta-\omega)r^2 - r^5\omega^2)\sin 2\theta = 0.\end{aligned} \tag{6}$$

Looking at the second equation in (6) we notice that the roots of this system can be divided into two types depending on the value of θ: the ones corresponding to $\sin 2\theta = 0$ or the ones associated to $-3J_2 + 2\delta(\beta-\omega)r^2 - r^5\omega^2 = 0$ with $\sin 2\theta \neq 0$. On the one hand if $\sin 2\theta = 0$, we have to consider two different situations, either $\theta = 0$ or $\theta = \pi/2$. If $\theta = 0$, then $\rho = 0$ and the dust grains are placed symmetrically on the z-axis at a distance of $\sqrt{3J_2}$ whenever $J_2 > 1/3$, in order to get a meaningful solution lying outside the planet. If $\theta = \pi/2$ we have equatorial orbits. On the other hand, when $\theta \neq \pi/2$, we obtain the halo orbits.

Note that the values of the parameters β and J_2 are fixed for a given planet. Thus, the occurrence of equatorial and halo orbits depends on the values of δ and ω.

4. Existence of equatorial orbits

As it was said above, equatorial orbits appear when $\theta = \pi/2$. In this case the second equation of (6) vanishes, and r must satisfy the polynomial equation

$$3J_2 + 2(1 - \beta\delta + \delta\omega)r^2 - 2\omega^2 r^5 = 0. \tag{7}$$

Then, the occurrence of equatorial orbits is reduced to the existence of positive real roots of (7). We note that this equation, for $\delta = 0$, reduces to a quadratic polynomial equation in r, provided that now $\omega = P_\phi/r^2$. Indeed, we have

$$2r^2 - 2P_\phi^2 r + 3J_2 = 0,$$

which gives rise to the equatorial orbits reported by Langbort [17].

For $\delta \neq 0$, we first note that if $\omega = 0$ Eq. (7) is regarded as a second degree polynomial equation in r with a positive real root if and only if $J_2(1 - \beta\delta) < 0$. As a consequence, for the oblate case ($J_2 > 0$) we have equatorial orbits if $\beta\delta > 1$ and for the prolate case ($J_2 < 0$) if the inequality is the opposite, that is $\beta\delta < 1$.

In the general case ($\omega \neq 0$), Descartes rule of signs [21] shows, as previously, that the prolate and oblate cases are different.

On the one hand, for the prolate case ($J_2 < 0$), it follows that Eq. (7) has no positive real roots for $(\beta - \omega)\delta \geqslant 1$, as there are no changes in the sequence of signs in the coefficient list. Nevertheless, when $(\beta - \omega)\delta < 1$ the sequence of signs presents two changes, thus there are none or two positive real roots. The limit curve dividing the plane δ–ω into two regions with none or two positive real roots can be obtained from the discriminant of the polynomial in (7) and it is given by

$$3125J_2^3\omega^4 + 32(1 - \beta\delta + \delta\omega)^5 = 0. \tag{8}$$

On the other hand, for the oblate case ($J_2 > 0$) the number of sign changes in the coefficient list is one. Thus, Eq. (7) has a positive real root. This means that regardless of the values of ω and δ, there is always an equatorial orbit.

Note that the scenario of existence of equatorial orbits for $J_2 \neq 0$ is modified from that of the case $J_2 = 0$ (for more details see [4]), where the existence of one equatorial orbit is constrained to a certain region of the plane δ–ω whose boundary is given by the curve

$$(\beta - \omega)\delta = 1, \tag{9}$$

which can be obtained from (8) by taking $J_2 = 0$.

It is interesting to discuss the existence curve of equatorial orbits, given by (8), for $J_2 \leqslant 0$ in terms of β and J_2. Indeed, for $J_2 = 0$, Eq. (9) is the standard hyperbola $\omega = -1/\delta$ displaced β units along the ω-axis. However, if $J_2 < 0$, Eq. (8) is no longer a hyperbola, although it is still a two-branched curve with the same asymptotic lines as (9). The disposal of the two branches depends on the values of J_2 and β. Thence, if β is fixed, there is a critical value of J_2, namely

$$J_2^c = -\sqrt[3]{\frac{32}{3125\beta^4}}$$

such that if $J_2^c < J_2 < 0$ the left branch of the curve is above the horizontal asymptotic line $\omega = \beta$, whereas the right branch is below it. The curve resembles the case $J_2 = 0$. On the contrary, if $J_2 < J_2^c < 0$ the left branch is now below the line $\omega = \beta$, whereas the right branch is above it. In the limit case, $J_2 = J_2^c$, the two branches intersect at the point $(4/(5\beta), \beta)$ and one of the branches is precisely $\omega = \beta$, as it can be seen in Fig. 1. It is worth noting that all the limit curves, regardless of the value of $J_2 < 0$, have the point $(1/\beta, 0)$ in common, which is a cuspidal point. Moreover, the region of existence of equatorial orbits is given by the condition

$$3125J_2^3\omega^4 + 32(1 - \beta\delta + \delta\omega)^5 > 0$$

and it gets smaller as J_2 decreases.

If we fix now the value of J_2, the situation is similar to that discussed above. There is a critical value of β in such a way that the disposal of the two branches of the curve changes with respect to the asymptotic lines (see Fig. 2). We note now that all the curves intersect at the points

$$\left(0, \pm\sqrt[4]{\frac{-32}{3125J_2^3}}\right),$$

and the region of existence of equatorial orbits is modified in a different way, depending on the sign of δ. In fact, if $\delta > 0$, the region of existence is smaller for increasing values of β. However, if $\delta < 0$ the region of existence is bigger for increasing values of β.

By now, we see that the oblateness of the body affects the region of existence of equatorial orbits in the plane δ–ω. In this way, it does not matter how oblate the body is, there always exists an orbit with fixed values of δ and ω (except for the limit case $\omega = 0$). For a spherical body, the region for equatorial orbits is no longer the whole plane, and a limit boundary appears in such a way that, inside this region, an equatorial orbit exists for fixed values of δ and ω. Finally, for a prolate body, the region of existence diminishes as J_2 decreases, but now, for fixed values of δ and ω within the region, there exist two equatorial orbits.

Beyond the existence of equatorial orbits, we have to pay attention to the radius of the orbit in the sense that if $r < 1$ the orbit would lie inside the planet and it constitutes a meaningless situation. In this way, the effective boundary for the existence of equatorial orbits is obtained by making $r = 1$ in Eq. (7), that is

$$2 - 2\beta\delta + 3J_2 + 2\delta\omega - 2\omega^2 = 0. \tag{10}$$

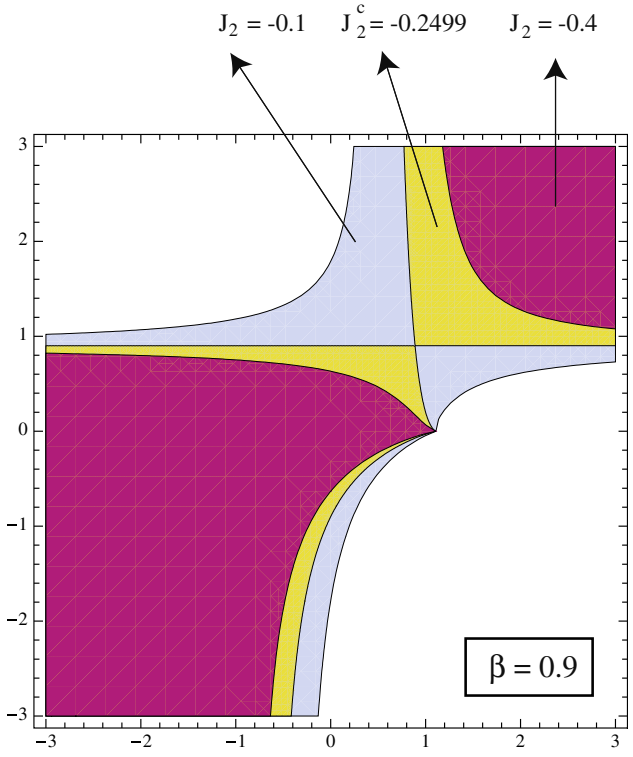

Fig. 1. Boundaries for the existence of equatorial orbits in the plane δ–ω for $\beta = 0.9$ and different values of J_2 for the prolate case.

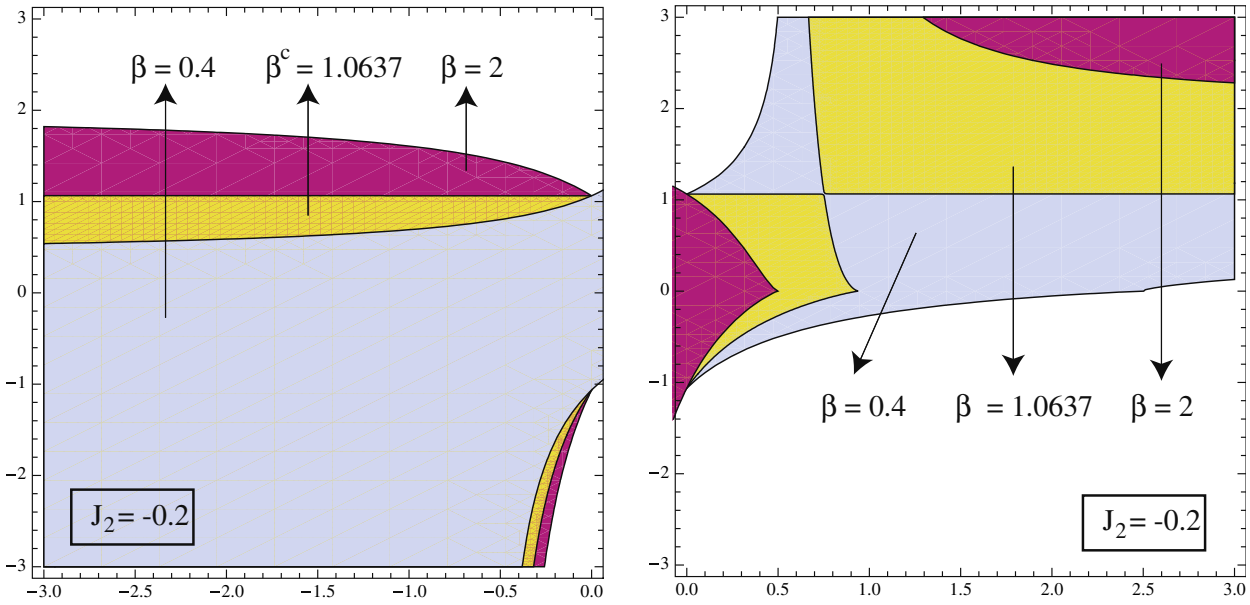

Fig. 2. Boundaries for the existence of equatorial orbits in the plane δ–ω for $J_2 = -0.2$ and different values of β for the prolate case.

Then, the region for orbits with $r \geqslant 1$ is defined by

$$2 - 2\beta\delta + 3J_2 + 2\delta\omega - 2\omega^2 \geqslant 0.$$

Eq. (10) defines a hyperbola whose asymptotic lines are $\omega = \beta$ and $\omega = \delta - \beta$. If J_2 and β satisfy the relation

$$3J_2 + 2 - 2\beta^2 = 0,$$

then the two branches of the hyperbola are precisely the two asymptotic lines. Moreover, if we fix a value of β and vary the value of J_2 the limit curves do not cut each other and the region of admissible equatorial orbits diminishes as J_2 decreases as it is depicted in the upper part of Fig. 3. Thus, the oblateness favors the existence of equatorial orbits. However, if we fix J_2 and vary β all the curves intersect at the points

$$\left(0, \pm\sqrt{1 + \frac{3}{2}J_2}\right),$$

in such a way that the region enlarges for $\delta > 0$ and decreasing β and the opposite for $\delta < 0$, that is, the region enlarges for increasing β (see the lower part of Fig. 3).

Nevertheless, we recall that in the prolate case ($J_2 < 0$), although the existence region is smaller, for fixed β, there are two equatorial orbits associated to each of the allowed parameters' values.

Now the question is whether there is a region where the two orbits have $r > 1$ at the same time or not. To solve this question, we note that orbits appear by pairs when a double root takes place. As a consequence, the region we are looking for must be delimited by the existence curve given by (8) and by the effective existence curve given by (10). The resultant of the two polynomials in (8) and (10),

$$32(\beta - \omega)^5(J_2 + \omega^2)^2(243J_2^3 - 1296J_2^2\omega^2 + 304J_2\omega^4 - 32\omega^6) = 0,$$

gives us the contact points between both pairs of curves.

No factors except for $(J_2 + \omega^2)^2$ yield to valid solutions. Then, the two pairs of curves (8) and (10) are tangent at the points

$$(\delta, \omega) = \left(\frac{-2 - 5J_2}{2(-\beta \pm \sqrt{-J_2})}, \pm\sqrt{-J_2}\right).$$

As a consequence, the region for two equatorial orbits is delimited by (8) and (10) between the two contact points. However, this region depends on the relative values of β and J_2. Indeed, we note that if $J_2 = -\beta^2$ the tangent points go to infinity and the region must change after this value is reached. The region also changes with the critical values of J_2 as it can be seen in Figs. 4 and 5 where a global evolution of the limit curves for a prolate body is depicted for $\beta = 0.9$ and $\beta = 0.5$ in terms of J_2.

The situation described above can be understood if we pay attention to the set of equatorial orbits of constant r. This set is a family of hyperbolas in the δ–ω plane, with asymptotic straight lines given by

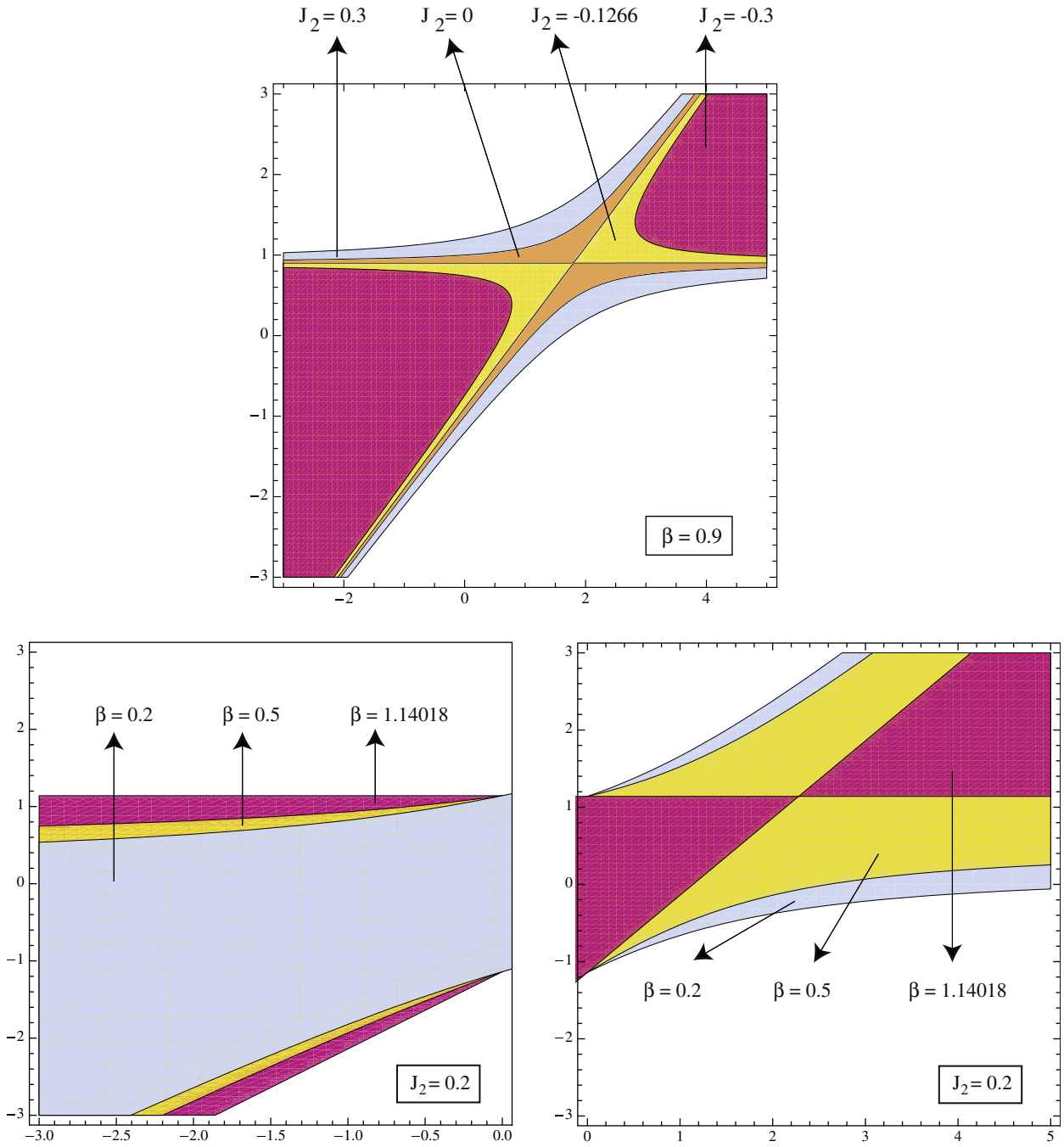

Fig. 3. Boundaries for the effective existence of equatorial orbits in the plane δ–ω: (top) for $\beta = 0.9$ and varying J_2; (bottom) for $J_2 = 0.2$ and different values of β.

$$\omega = \beta, \quad \omega = \frac{\delta}{r^3} - \beta.$$

Moreover, the curves of constant radius, for a fixed β, do not touch each other if $J_2 > 0$, all of them are tangent at $(1/\beta,0)$ if $J_2 = 0$ and every pair of curves cut each other twice for $J_2 < 0$. This is the reason why the prolate case is more intricate than the oblate one. Besides, we note that the asymptotic straight lines of the family correspond to the radius of the synchronous orbit (r_s) obtained by setting $\omega = \beta$ (the frequency of the synchronous orbit). Once again the prolate case differs from the oblate one. On the one hand, for $J_2 > 0$, r_s is the positive solution of the equation

$$2\beta^2 r^5 - 2r^2 - 3J_2 = 0, \tag{11}$$

and we stress that now r_s is not given by Kepler's third law $\beta^2 r^3 = 1$, but by a modified one. We can express it asymptotically in terms of J_2 as

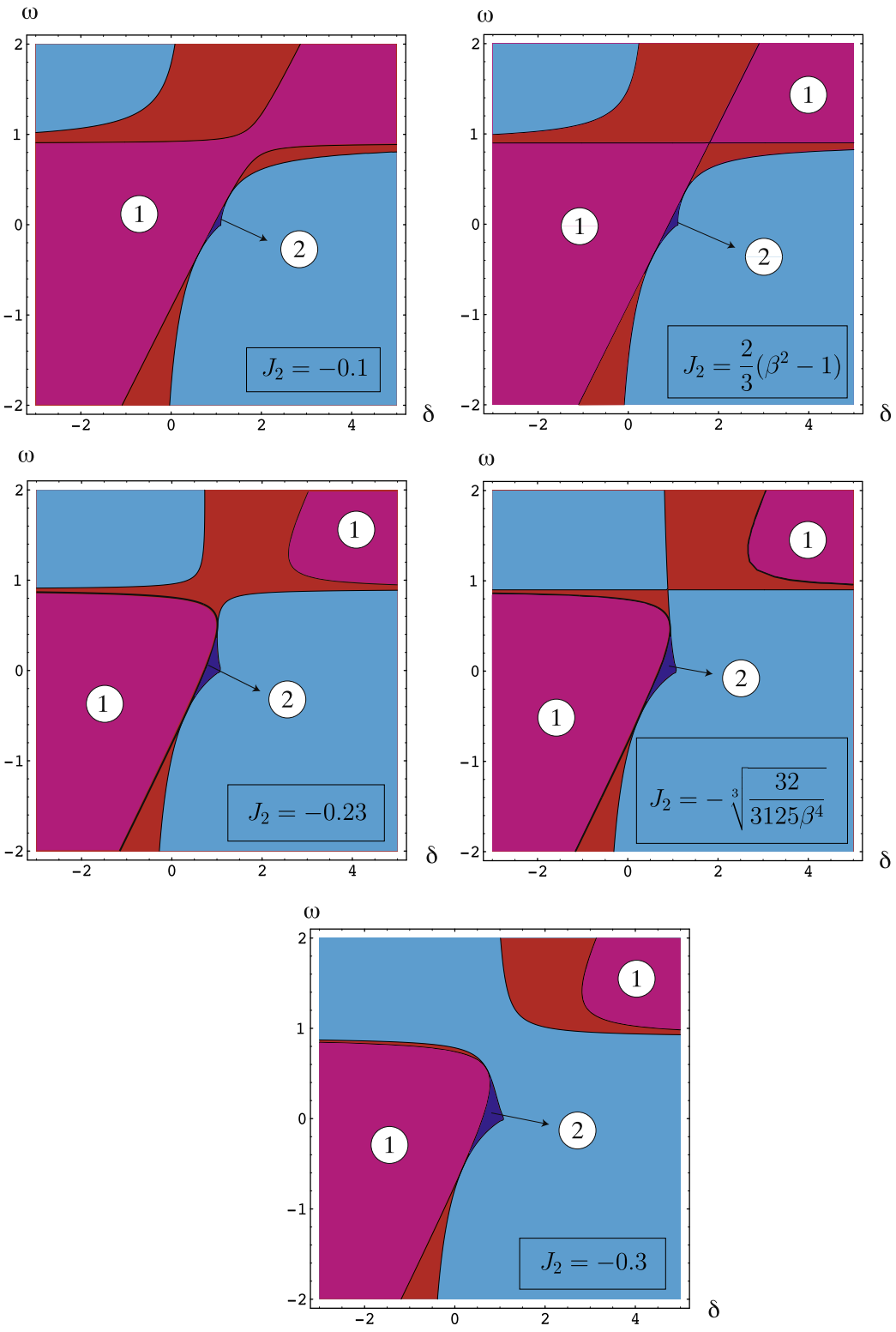

Fig. 4. The regions of existence and effective existence of equatorial orbits for different prolate bodies and $\beta = 0.9$. Encircled is the number of equatorial orbits.

$$\beta^2 r^3 = 1 + \frac{3}{2}\beta^{4/3} J_2 - \frac{3}{2}\beta^{8/3} J_2^2 + O(J_2^3).$$

The most remarkable fact is that the synchronous orbit plays the role of a separatrix in the sense that if $r > r_s$ there is a closed interval of non-allowed charge–mass ratio values, but all the frequencies are possible (see Fig. 6). Indeed, those particles with δ belonging to the interval $[\delta_-, \delta_+]$, with

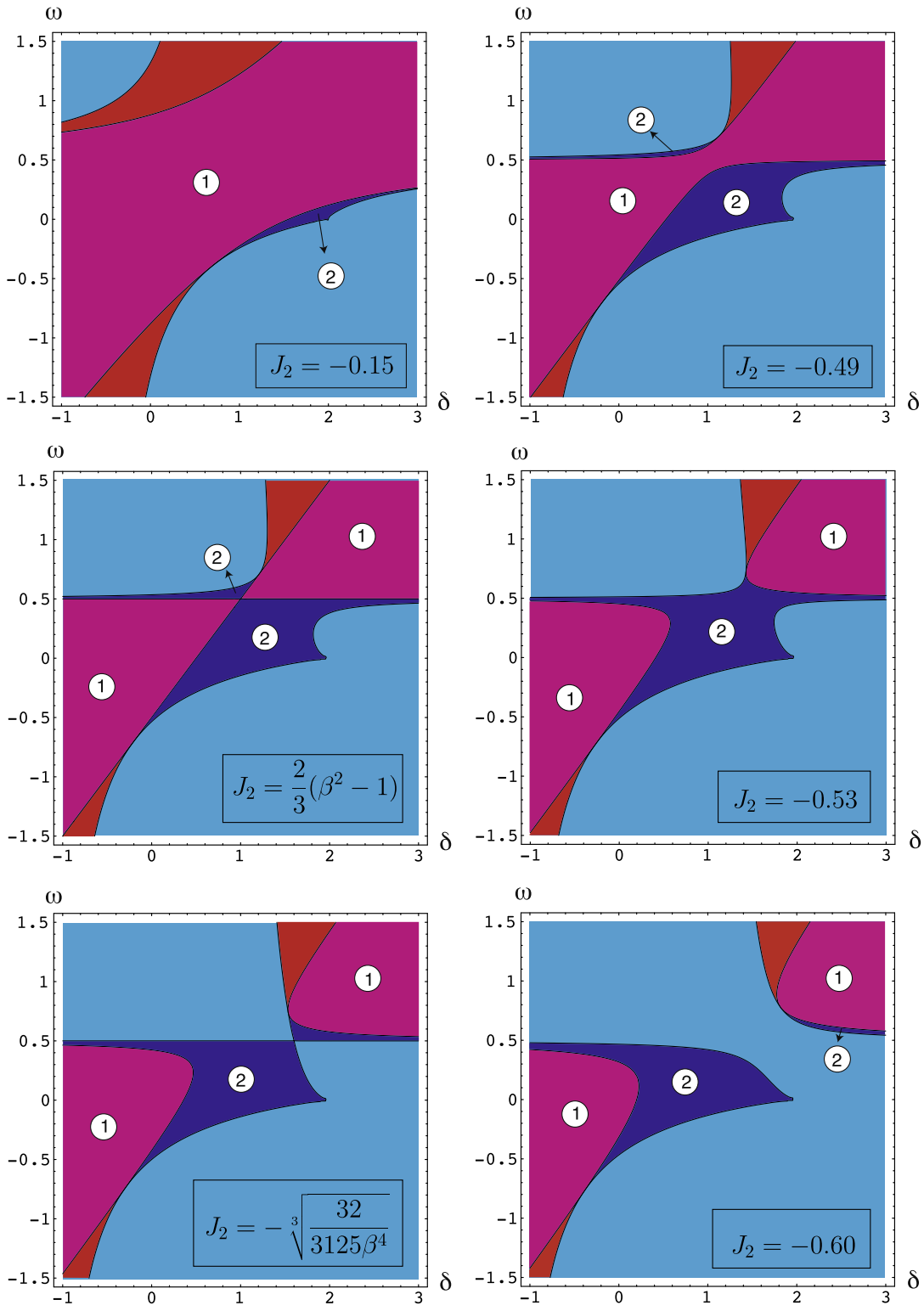

Fig. 5. The regions of existence and effective existence of equatorial orbits for different prolate bodies and $\beta = 0.5$. Encircled is the number of equatorial orbits.

$$\delta_{\pm} = 2\beta r^3 \pm \sqrt{2r(2\beta^2 r^5 - 2r^2 - 3J_2)}, \tag{12}$$

are not allowed to be in an equatorial orbit of radius r. Notice that the expression in the square root in (12) is related with the radius of the synchronous orbit given by (11), in such a way that if $r > r_s$ the expression is positive and negative if $r < r_s$. Besides, as r tends to infinity, δ_- approaches $1/\beta$, whereas δ_+ goes to infinity. As a consequence, as r increases, more and more particles are swept from equatorial orbits if their charge–mass ratio is greater than $1/\beta$.

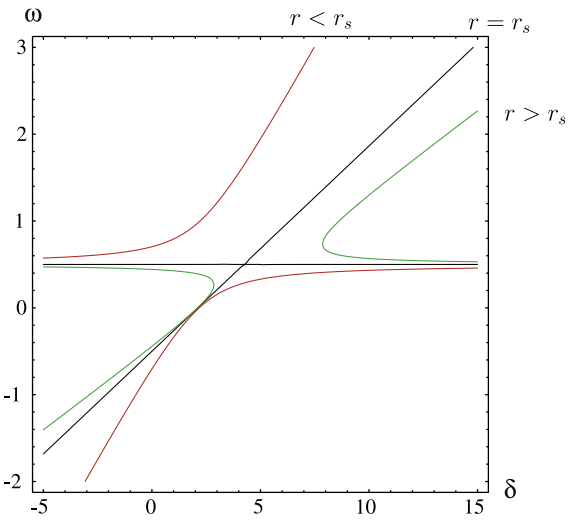

Fig. 6. Curves of constant radius for equatorial orbits with $J_2 = 0.1$ and $\beta = 0.5$.

On the other hand, for $J_2 < 0$, two synchronous orbits appear. One of them is obtained as a perturbation of the synchronous orbit for the spheric case, $J_2 = 0$, and the other one as a consequence of the prolate shape of the body. Nevertheless, if the absolute value of J_2 is small enough, the second synchronous orbit lies inside the body. But if the values of J_2 and β satisfy the inequality

$$-\sqrt[3]{\frac{32}{3125\beta^4}} \leqslant J_2 \leqslant \frac{2}{3}(\beta^2 - 1),$$

and $\beta \leqslant \sqrt{2/5}$, the two synchronous orbits have $r \geqslant 1$ and are physically possible at the same time. For example, for $\beta = 0.5$ and $J_2 = -0.52$ there are synchronous orbits at $r = 1.0442$ and $r = 1.27925$.

Finally, we remark that the trajectories discussed through this section correspond to the circular equatorial orbits found in Iñarrea et al. [13–15] for $J_2 = 0$ using normalisation and reduction techniques. Furthermore, they are the same orbits as the ones encountered by Grotta-Ragazzo et al. [5] using P_ϕ as a parameter instead of ω.

5. Existence of halo orbits

Halo orbits appear as the solutions of system (6) when $\theta \neq \pi/2$. In this case, the term in r in the second equation of (6) must be zero, and then the following equation is satisfied

$$3J_2 + 2\delta(\omega - \beta)r^2 + \omega^2 r^5 = 0. \tag{13}$$

It is worth noting that for $\delta = 0$, $\omega^2 = P_\phi^2/r^4$, and Eq. (13) gets simplified to

$$3J_2 + P_\phi^2 r = 0.$$

Thus, halo orbits are obtained if $J_2 < 0$, according to the results in [17].

For $\delta \neq 0$, we proceed as in the equatorial case, first considering $\omega = 0$, as it acts as a limit case. Now, Eq. (13) reduces from a quintic to a quadratic one and at least one of the roots of (13) goes to infinity. This fact will provide further insight in the discussion of the existence of halo orbits. Let us note that (13), when $\omega = 0$, has a positive solution if

$$\delta J_2 > 0,$$

provided that $\beta > 0$. Thus, for an oblate body only positively-charged particles are suitable to be in halo orbit. On the contrary, for a prolate body, the admissible particles are those negatively-charged. However, the discrimination just made takes into account only one of the equations of system (6). We must impose that the other equation is satisfied, that is

$$-6J_2 + 2r^2 + (9J_2 - 2\delta\beta r^2)\sin^2\theta = 0. \tag{14}$$

Solving for $\sin^2\theta$, we get

$$\sin^2\theta = \frac{6J_2 - 2r^2}{9J_2 - 2\delta\beta r^2}.$$

Thence, we have a solution if

$$0 \leqslant \frac{6J_2 - 2r^2}{9J_2 - 2\delta\beta r^2} \leqslant 1.$$

But, taking $\omega = 0$ in (13) we get that $r^2 = 3J_2/(2\delta\beta)$ and, finally, we have a positive solution if

$$0 \leqslant \frac{1}{\delta\beta} \leqslant 2.$$

This implies that $\delta > 0$, and we obtain solutions only for an oblate body, as in the prolate case only negatively-charged particles could be in a halo orbit for $\omega = 0$.

In the general case, when $\omega \neq 0$, we will follow a similar procedure, that is, to find r from Eq. (13) and then to substitute this value into the first equation of (6) to obtain a value for $\sin^2\theta$ in the interval [0,1]. However, (13) being now a quintic polynomial equation it is not possible to obtain r in terms of the parameters.

Descartes rule of signs yields a different behavior for prolate and oblate cases. Indeed, if $J_2 < 0$, Eq. (13) has a unique positive real root. On the contrary, if $J_2 > 0$, Eq. (13) has none or two positive real solutions, depending on the values of δ and ω, fixed β and J_2. Taking into account the discriminant of the quintic, we have two positive real roots if and only if

$$128\delta^5(\beta - \omega)^5 - 3125J_2^3\omega^4 > 0. \tag{15}$$

However, Eq. (13) is not enough to ensure the existence of halo orbits. First equation of system (6) must be also satisfied. Therefore, obtaining J_2 from Eq. (13) and substituting its value in the first equation of system (6), we get

$$r^3\omega^2(5\sin^2\theta - 2) - 2[1 + 2\delta(\beta - \omega)(\sin^2\theta - 1)] = 0.$$

This is a linear equation in r^3 and $\sin^2\theta$. This means that each value of r is related with a unique value of $\sin^2\theta$ and vice versa. Thus, for a given r, i.e., a root of (13), we can obtain a halo orbit if

$$0 \leqslant \sin^2\theta = 1 - \frac{3\omega^2 r^3 - 2}{5\omega^2 r^3 + 4\delta(\omega - \beta)} \leqslant 1.$$

If this holds, two symmetric halo orbits respect to the equatorial plane occur.

The preceding condition can be expressed in terms of δ, β, ω and θ by elimination of r in system (6), arriving at the following equation in $\sin^2\theta$:

$$32[-1 + 3\delta(\beta - \omega)\sin^2\theta]^3[1 - 2\delta(\beta - \omega)(1 - \sin^2\theta)]^2 - 27J_2^3\omega^4(5\sin^2\theta - 2)^5 = 0. \tag{16}$$

Now it is easy to find the limit curves for an admissible value of $\sin^2\theta$, by substitution of $\sin^2\theta = 1$ and $\sin^2\theta = 0$ in (16). Thus, we find

$$\sin^2\theta = 1 \rightarrow 32[-1 + 3\delta(\beta - \omega)]^3 - 6561J_2^3\omega^4 = 0, \tag{17}$$

$$\sin^2\theta = 0 \rightarrow 864J_2^3\omega^4 - 32[1 - 2\delta(\beta - \omega)]^2 = 0. \tag{18}$$

These two curves lie in the area of the plane δ–ω where the polynomial Eq. (13) has positive real roots.

Let us look more carefully what happens for the prolate and oblate cases. If $J_2 < 0$, only the limit curve (17) must be taken into account, provided there is no restriction for the existence of positive real roots of the polynomial equation (13), and (18) does not produce any limit curve. By fixing β and varying J_2, it is seen that the region of halo orbits in the plane δ–ω increases as J_2 diminishes. This situation still remains if we consider those orbits with $r > 1$, as it is depicted in Fig. 7. If we fix now J_2 and vary β, the region of admissible halo orbits with $r > 1$ behaves differently for positively and negatively charged particles, as it also happened for equatorial orbits. In this sense, the region diminishes for increasing β if the particle is negatively charged, and for positively charged particles the region enlarges for increasing β (see Fig. 8). Note that this is the opposite behavior observed for equatorial orbits in the prolate case.

For the oblate case the situation is more complicated, as the three limit curves must be taken into account. They are tangent at the points (δ_t, ω_t) given by

$$\delta_t = \frac{5}{6(\beta - \omega_t)}, \quad \omega_t^4 = \frac{4}{243J_2^3}.$$

Moreover, it can be observed that, fixing β, the region of admissible halo orbits ($r > 1$) diminishes as J_2 increases (see Fig. 9). As a consequence, there exists a range of charge–mass ratios not allowed for particles to be in a halo orbit. This range depends on β and J_2 and it is bounded for the negative and positive real roots of the equation

$$\delta^4 + 72\beta J_2\delta - 24J_2^3 = 0.$$

For example, in the case of Saturn, we have $\beta = 0.4$ and $J_2 = 0.016298$, and those particles such that

$$\delta \in [-0.777231, 0.000221354]$$

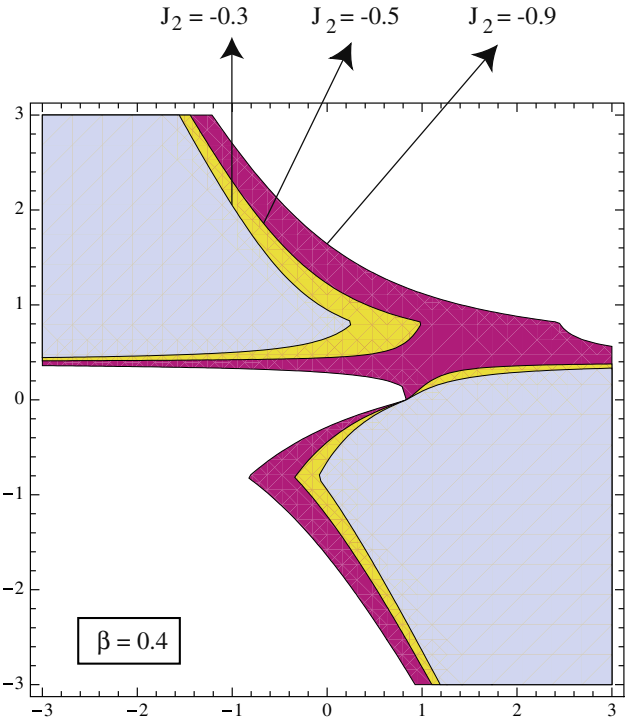

Fig. 7. Regions of existence of halo orbits in the prolate case with $r > 1$, fixing β and varying J_2.

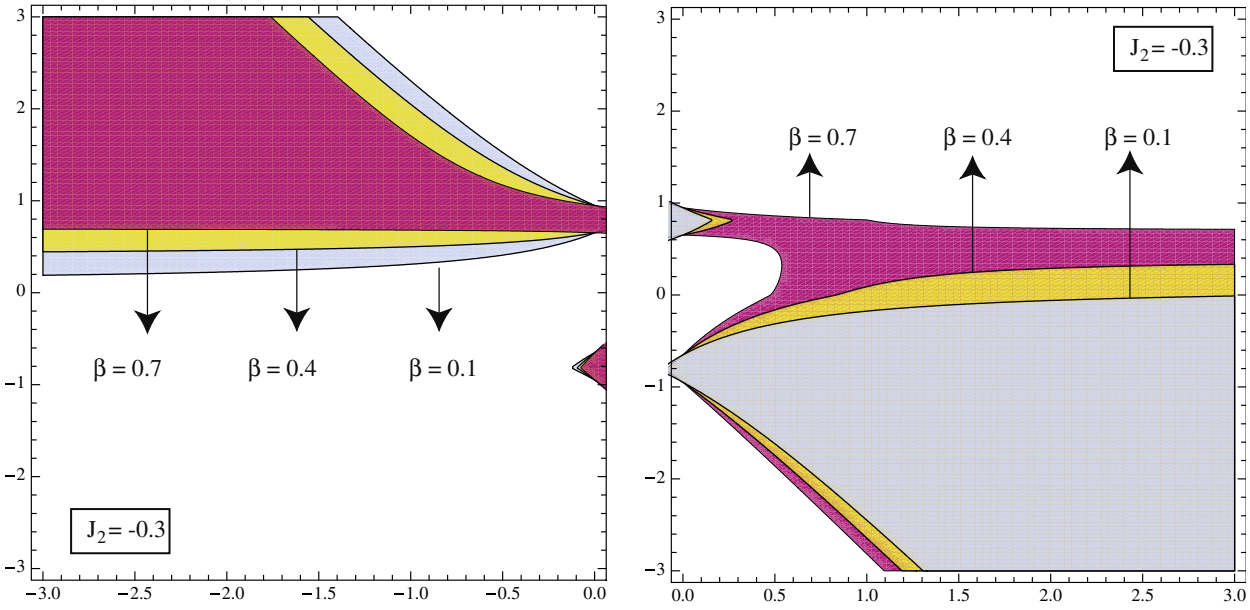

Fig. 8. Regions of existence of halo orbits in the prolate case with $r > 1$, fixing J_2 and varying β.

cannot be in a halo orbit. This implies that oblateness prevents low charged particles, specially those negative charged, to orbit away the equatorial plane. For spherical dust particles of radius a, uniform density ρ and potential Φ, the parameter δ can be written as

$$\delta = \frac{\omega_c}{w_k} = \frac{3\Phi B_0}{4\pi k_e a^2 \rho w_c},$$

where B_0 is the magnetic field strength of the planet on the equator and k_e is the Coulomb electrostatic constant. If we consider a typical icy micron-sized particle ($a = 1$ μm and $\rho = 1$ g/cm^3) around Saturn ($B_0 = 0.210$ G and $w_k = 4.160 \times 10^{-4}$ rad/s), parameter δ only depends on the potential Φ. If we also assume that the potential varies from -10 to 5 V, for particles at distances between 2 and 8 planetary radius [3], we have

$$\delta = 0.00133887\Phi \in [-0.0133887, 0.00669433]$$

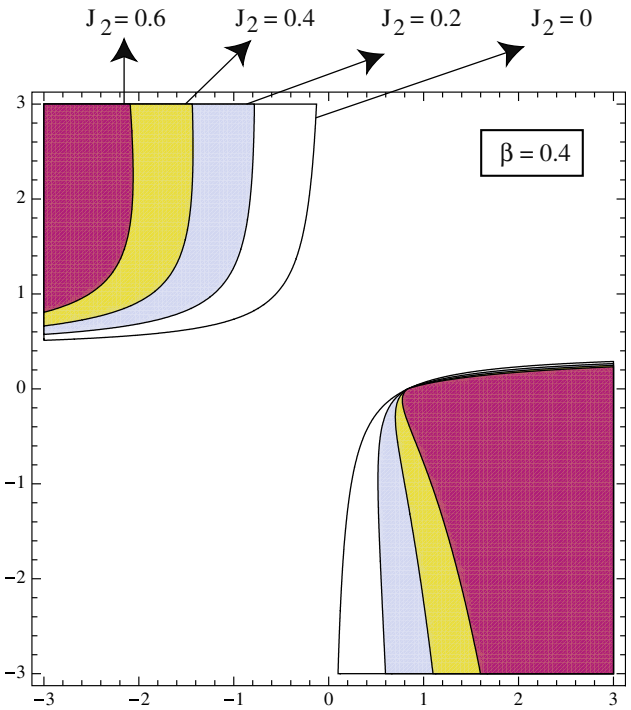

Fig. 9. Regions of existence of halo orbits in the oblate case, fixing β and varying J_2.

and, only those particles such that $\Phi > 0.16533$ can be in a halo orbit. However, if the size of the particle is ten times smaller, we can have particles in a halo orbit if $\Phi < -5.8$ or $\Phi > 0.0016533$.

Now, we fix J_2 and vary the parameter β. Then, the region of admissible orbits enlarges for positive charged particles as β increases. On the contrary, the region diminishes as β increases for negative charged particles (see Fig. 10). It is worth noting that bigger values of β favor positively charged particles, whereas small values favor negatively charged ones.

The discussion above, for the oblate case, only takes into account the existence of, at least, one halo orbit, regardless the radius of it. Obviously, if a lower bound is imposed to the radius, the region of existence turns to be smaller. Moreover, the question of the existence of two halo orbits has not been faced till now. Let us go to this problem trying to demonstrate that two halo orbits with $r > 1$ can occur at the same time for suitable values of β and J_2. To this end, we need the results obtained for the case $\omega = 0$. In this case, we got one of the halo orbits at infinity, whereas the other one got a radial distance given by

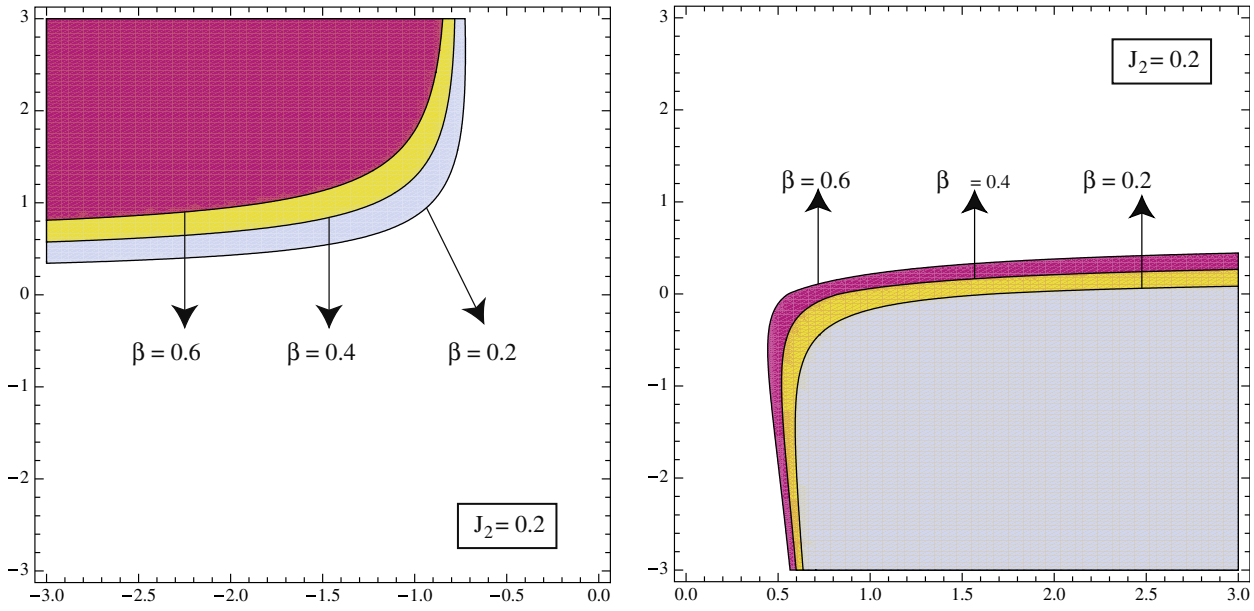

Fig. 10. Regions of existence of halo orbits in the oblate case, fixing J_2 and varying β.

$$r = \frac{3J_2}{2\delta\beta},$$

provided $1/(2\delta\beta) \leqslant 1$. This implies that if $J_2 > 1/3$, two halo orbits with $r > 1$ are possible in a vicinity of $\omega = 0$. Fig. 11 shows a thin region where two halo orbits with $r > 1$ exist at the same time, for $J_2 = 0.4$ and $\beta = 0.5$.

However, the lower bound $r = 1$ is too restrictive, because the body is not spherical. In fact, depending on the shape of the body, the lower bound for the radius is a function of the latitude θ. For instance, if we assume that the body is a homogeneous ellipsoid of revolution with semimajor axis equal to one and semiminor axis equal to b, the radius r_h of the halo orbit must satisfy

$$r_h \geqslant \frac{b}{\sqrt{\cos^2\theta + b^2\sin^2\theta}}. \tag{19}$$

Besides, J_2 can be expressed in terms of the moments of inertia [8] as

$$J_2 = \frac{2C - A - B}{2M},$$

where A, B and C are the principal moments of inertia and M the total mass of the body. Taking into account that $A = B = (1 + b^2)M/5$ and $C = 2\ M/5$, it results in

$$J_2 = \frac{1}{5}(1 - b^2). \tag{20}$$

Note that J_2 cannot be greater than 1/5, a value less than the critical value obtained for J_2 in order to have two halo orbits with radius greater than one. The question now is if it is possible to have two admissible halo orbits, that is satisfying (19) provided J_2 is given by (20). The answer is yes, but for very oblate bodies. The procedure to arrive at this answer is analogous to the determination of the boundaries for the existence region of equatorial and halo orbits. By using the equation of the ellipsoid we have a relation between r, θ and the semiminor axis, or equivalently J_2. This yields

$$\sin^2\theta = \frac{r^2 + 5J_2 - 1}{5J_2 r^2}.$$

Substitution of this expression into the first equation of (6) gives

$$J_2^2(45 - 30r^2) + J_2(-9 + 10r^4 - 10r^5\omega^2 + r^2(9 - 10\beta\delta + 10\delta\omega)) - 2r^2(-1 + r^2)(\beta\delta + w(-\delta + r^3\omega)) = 0.$$

At this point, note that (6) is a system of polynomial equations in r. The resultant of them gives the condition for the existence of two halo orbits combined with (17) and (18). An inspection of these conditions shows that the relative position of the limit curves does not depend on β but only on J_2. Furthermore, if $J_2 = 1/8$ the limit curve obtained from the ellipsoid and the other one given by (18) turn to be the same. Thus, if $J_2 < 1/8$ only one or none halo orbits are possible. However, if $J_2 > 1/8$ there is a region, in most cases a thin region, where two halo orbits exist at the same time. For instance, in Fig. 12 it is de-

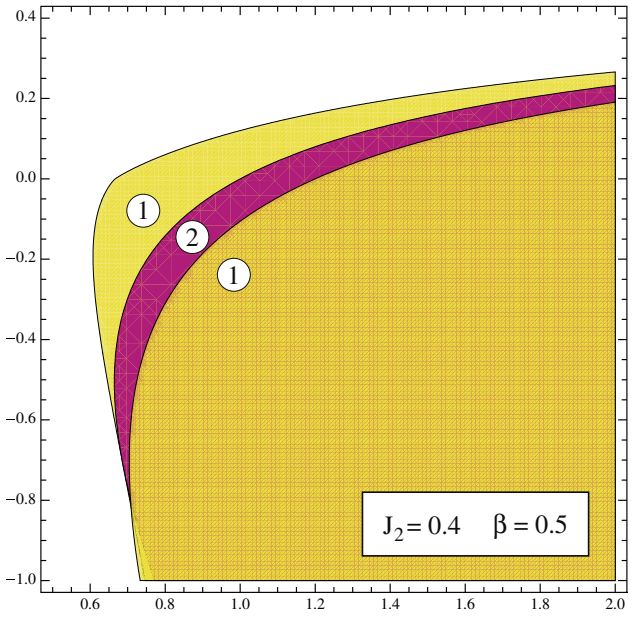

Fig. 11. The dark area corresponds to the region where two halo orbits with $r > 1$ exist. Encircled is the number of halo orbits with $r > 1$.

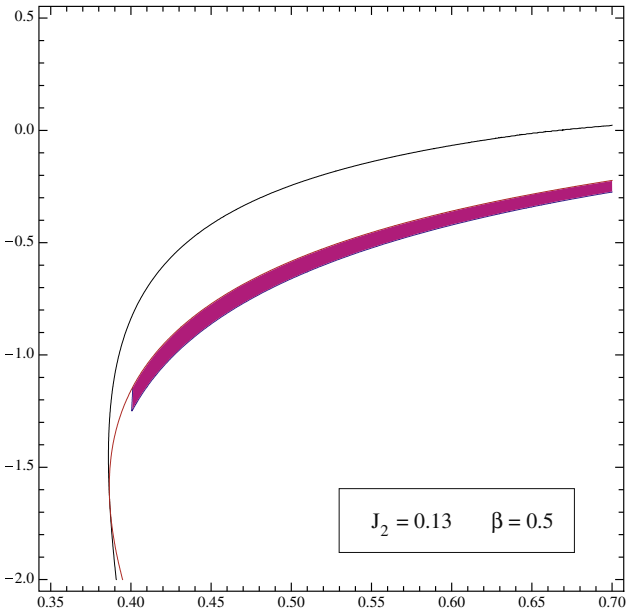

Fig. 12. The dark area corresponds to the region where two admissible halo orbits exist for a homogeneous ellipsoid of revolution in the case of $J_2 = 0.13$.

picted the region where two halo orbits appear for the selected parameters $\beta = 0.5$ and $J_2 = 0.13$, which implies a semiminor axis $b = 0.5916$. We stress that this value of J_2 is close to the oblateness coefficient of some asteroids, as 22 Kalliope with $J_2 \approx 0.127$ [18].

6. Conclusions

We have studied the occurrence of equatorial and halo periodic orbits of charged particles around a magnetic planet, where the perturbations taken into account include the gravity potential with the oblateness coefficient. Our analysis generalises the works [4,17] and exhibits a richer dynamics due to the effect of the oblateness of the planet.

The oblateness coefficient plays an important role on the existence of these kind of orbits. In fact, the character of the body, oblate or prolate yields different behavior, which is stated in the plane δ–ω. In this way, for an oblate body, there always exists an equatorial orbit. However physical real meaningful orbits do not exist in all cases. Nevertheless, all frequencies and all charge–mass ratios are suitable for equatorial orbits. The situation is more subtle for prolate bodies where, in some situations, depending on critical values of J_2 and β, particles with certain charge–mass ratios are swept from equatorial orbits. Besides, two equatorial orbits with different radius can share the same type of particles with the same frequency.

For halo orbits the situation is similar, but the role played for the oblateness is the opposite. For prolate bodies only one halo orbit appears inside a certain region, without no restriction on the charge–mass ratio. On the contrary, for an oblate body, we have observed that, as soon as the value of J_2 grows up, the range of particles swept from halo orbits increases. Besides, two halo orbits at different latitude are possible if the body is oblate enough.

The reason to consider bodies with very big oblateness coefficients is twofold. On the one hand it serves to highlight the effect of J_2 contributing to make clear the differences with the spherical case, as it was made similarly by other authors [2]. On the other hand, the analysis carried out in the paper may be of interest for the dynamics of charged grains around asteroids, as these dust particles can damage the solar panels of a spacecraft orbiting a certain asteroid [19].

Finally, our approach can be helpful for the analysis of the structure and composition of the planetary rings. For instance, it could be of interest in the study of Saturn's largest ring, the E ring. In this respect, we mention one of the experiments of the Cassini-Huygens mission, which consists in the analysis of the three-dimensional structure and dynamic behavior of the rings of Saturn and, in particular, the case of the E ring [16,24].

Acknowledgement

We thank financial support from Ministerio de Educación y Ciencia (Project # MTM2005-08595) from Spain.

References

[1] Campbell JK, Anderson JD. Gravity field of the Saturnian system from Pioner and Voyager tracking data. Astron J 1989;97:1485–95.
[2] Danby JMA. Motion of a satellite of a very oblate planet. Astron J 1968;73:1031–8.
[3] Dikarev VV. Dynamics of particles in Saturn's E ring: effects of charge variations and the plasma drag force. Astron Astrophys 1999;346:1011–9.
[4] Dullin HR, Horányi M, Howard JE. Generalizations of the Størmer problem for dust grain orbits. Physica D 2002;171:178–95.

[5] Grotta-Ragazzo C, Kulesza M, Salomão PAS. Equatorial dynamics of charged particles in planetary magnetospheres. Physica D 2007;225:169–83.
[6] Hamilton DP. Motion of dust in a planetary magnetosphere: orbit-averaged equations for oblateness, electromagnetic and radiation forces with application to Saturn's E ring. Icarus 1993;101:244–64. Erratum, Icarus, 103, 161, 1993..
[7] Hamilton DP, Krivov AV. Circumplanetary dust dynamics: effects of solar gravity, radiation pressure, planetary oblateness, and electromagnetism. Icarus 1996;123:503–23.
[8] Heiskanen WA, Moritz H. Physical geodesy. San Francisco: Freeman; 1967.
[9] Horanyi M, Burns JA, Hamilton DP. The dynamics of Saturn's E ring particles. Icarus 1992;97:248–59.
[10] Howard JE, Horányi M, Stewart GR. Global dynamics of charged dust particles in planetary magnetospheres. Phys Rev Lett 1999;83:3993–6.
[11] Howard JE, Dullin HR, Horányi M. Stability of halo orbits. Phys Rev Lett 2000;84:3244–7.
[12] Howard JE, Horanyi M. Nonkeplerian dust dynamics at Saturn. Geophys Res Lett 2001;28:1907–10.
[13] Iñarrea M, Lanchares V, Palacián J, Pascual AI, Salas JP, Yanguas P. The Keplerian regime of charged particles in planetary magnetospheres. Physica D 2004;197:242–68.
[14] Iñarrea M, Lanchares V, Palacián J, Pascual AI, Salas JP, Yanguas P. Global dynamics of dust grains in magnetic planets. Phys Lett A 2005;338:247–52.
[15] Iñarrea M, Lanchares V, Palacián J, Pascual AI, Salas JP, Yanguas P. Reduction of some perturbed Keplerian problems. Chaos, Solitons & Fractals 2006;27:527–36.
[16] Kempf S, Beckmann U, Srama R, Horanyi M, Auer S, Grün E. The electrostatic potential of E ring particles. Planetary Space Sci 2006;54:967–87.
[17] Langbort C. Bifurcation of relative equilibria in the main problem of artificial satellite theory for a prolate body. Celest Mech Dyn Astr 2002;84:369–85.
[18] Marchis F, Descamps P, Hestroffer D, Berthier J, Vachier F, Boccaletti A, et al. A three-dimensional solution for the orbit of the asteroidal satellite of 22 Kalliope. Icarus 2003;165:112–20.
[19] McCoy TJ, Robinson MS, Nittler LR, Burbine TH. The Near Earth Asteroid Rendezvous mission to asteroid 433 Eros: a milestone in the study of asteroids and their relationship to meteorites. Chemie der Erde – Geochemistry 2002;62:89–121.
[20] Murray CD, Dermott SF. Solar system dynamics. Cambridge: Cambridge University Press; 1999.
[21] Stoer J, Bulirsch R. Introduction to numerical analysis. New York: Springer; 1983.
[22] Størmer C. Sur les trajectories des corpuscules électrisés dans l'espace sous l'action du magnetisme terrestre avec application aux aurores boréales. Arch Sci Phys Nat 1907;24:5–18, ibid 113–158, ibid 221–247.
[23] Størmer C. The polar aurora. Oxford: Clarendon Press; 1955.
[24] Wang Z, Gurnett DA, Averkamp TF, Persoon AM, Kurth WS. Characteristics of dust particles detected near Saturn's ring plane with the Cassini Radio and Plasma Wave instrument. Planetary Space Sci 2006;54:957–66.